

Optimal Design of B-pillar of Tailor-welded Blank Structure Considering Crashworthiness and Light-weighting

Tan Yaowu, Yang Jikuang

(State Key Laboratory of Advanced Design and Manufacture for Vehicle Body, Hunan University, Changsha, 410082, China)

Abstract: The present paper aims to get a desired deformation mode of a vehicle's B-pillar in side impact to enhance crashworthiness and reduce the total mass. We developed a finite element model of side impact and validated it. We improved the tailor-welded blank structure of B-pillar by optimal design of the location of welded seam and thickness of this structure considering crashworthiness and light-weighting by using design of experiment method and multi-objective genetic algorithm. By such optimization we could reduce B-pillar maximum intrusion with 10.1%. The intrusion and intrusion velocity at the middle of B-pillar were reduced by 18.4% and 11.8%, respectively. The mass was reduced by 18.1%. The results indicate that optimal designing of tailor-welded blank structure can effectively balance the requirements of crashworthiness and light-weighting.

Keywords: crashworthiness, light-weighting, B-pillar, tailor-welded blank, optimal design

1 Introduction

Due to increasing legal and market demands for safety, the weight of a conventional car body will most likely increase in the future. For the other hand, environmental demands will become stronger than today and lowering the vehicle weight will play an important role^[1]. Therefore, improvement of crashworthiness of car body structure and light-weighting are usually incompatible. This subject becomes a hot issue in the studies done by automobile industry. One of the promising approaches to meet these two requirements is to use a tailor-welded blank (TWB) structure^[2].

Tailor-welded blank is a panel consisting of two or more sheets with different mechanical properties, coating types and thickness welded together in order to get a structure with desired strength and stiffness. Although the tailor-welded blank has been widely used in automobile industry, the designs of it mainly rely on the experience of experts or on reference to the existing ones. Only a few researchers made some quantitative studies. Shin *et al.*^[3] and Lee *et al.*^[4] determined the domains and thickness of the gauges of TWB in a front door structure by a series of optimizations. In their research, the variables were optimized separately. In another study by Song and Park^[5], carried out a multidisciplinary optimization of a TWB structure, in which the door stiffness, natural frequency and side impact safety were investigated. In their paper, the entire optimization system was divided into multiple domains solved separately and the response surface method was utilized to approximate the complex problem.

B-pillar is a major structural component in side impact safety, and its intrusion, intrusion velocity and deformation mode influence the injury of occupants^[6]. The current paper aims to get a desired deformation mode of B-pillar like a pendulum with its center of rotation located at the B-pillar to roof rail joint, as described in^[7], at the same time consider two requirements: improvement of crashworthiness and light-weighting. We used a tailor-welded blank structure to replace the original B-pillar structure, and then optimized its parameters such as location of welded seam and thickness using design of experiment (DOE) method and multi-objective genetic algorithm (GA).

2 Preparation for multi-objective optimization

2.1 Model development and validation

The available finite element (FE) model of the car, which was developed by the researchers in our laboratory, was selected to be used in simulation of side impact. A side impact FE model was built by using hypermesh according to the Chinese safety regulation—the protection of the occupants in the event of a lateral collision. It contains FE models of the car and mobile deformable barrier (MDB). In simulation, the MDB model was impacting the side of car vertically as shown in Figure 1 with the speed of 50 km/h. Besides, the simulation time was set to 0.01 second, because real impact time in the test was about 0.007second. The accuracy of simulation was validated by comparing time-histories of acceleration of the car body in side impact simulation with that in the test conducted at the same conditions. The two acceleration curves are shown in Figure 2. From the figure, we can see that the trend of acceleration curves is basically similar. Meanwhile, the corresponding peaks of the curves both in test and simulation appear almost at the same time. Although there is a certain difference of acceleration peak values in simulation and the test because we neglected some car body attachments. There were also differences of material parameters and simplification in spot-weld model during establishing the whole car FE model. However, the difference of acceleration peak values was less than 5%, so the FE model could be accepted in the following simulation analysis of side impact safety.

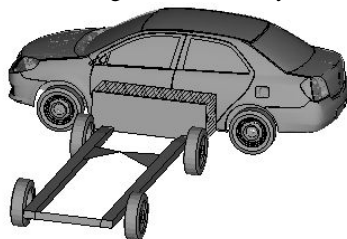


Figure 1. Side impact FE model

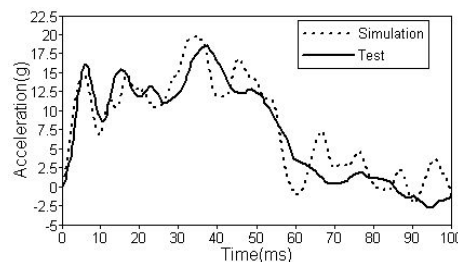


Figure 2. Acceleration curves of vehicle body in test and simulation

2.2 Vehicle structure in side impact – problem definition

Based on the same simulation used in the model validation we analyzed the safety performance by the deformation, intrusion

and intrusion velocity. From the simulation results, shown in Figure 3, we can see that the safety performance of the car body structure is not satisfactory, for the reasons that the side deformation was strongly concave, and the intrusion velocity is higher than 10 m/s. Meanwhile, some large deformation of roof and floor also occurred. Because the scope of current study was to optimize tailor-welded blank structure of B-pillar, we decided to modify the original car structure before the optimization process regarding material and property of sill, cross beam of roof, rear floor and side impact beam. The car structure showed somewhat better performance in side impact especially regarding deformation in the area of floor and roof as shown in Figure 7a. However, two problems of B-pillar structure still existed after this improvement:

a) The deformation mode of B-pillar was not satisfactory enough, because the mid-section of B-pillar deformed badly, and the intrusion velocity was too large. We know from literature that risk of human chest injury is in proportion to the intrusion velocity at the mid-section of B-pillar^[8];

b) B-pillar structure includes too many reinforcements, shown in Figure 4. It is not only bad for the light-weighting, but also increases the complexity of design process and assembly of vehicle body.

In order to solve the above two problems, we replaced the original B-pillar structure with a tailor-welded blank structure, and then optimized parameters such as location of welded seam and thickness using design of experiment (DOE) method and multi-objective genetic algorithm (GA).

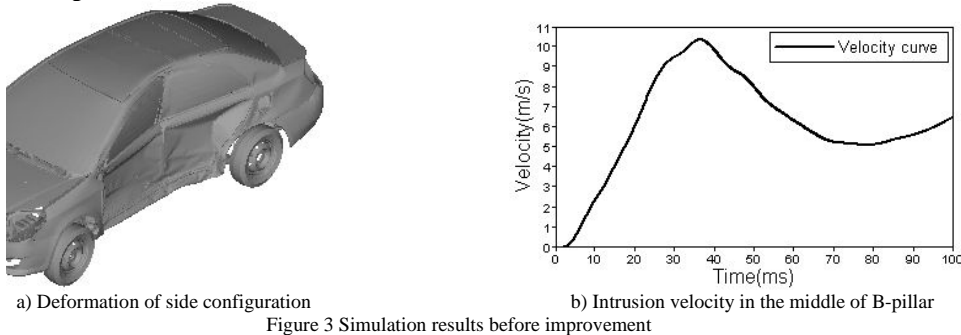


Figure 3 Simulation results before improvement

2.3 Tailor-welded blank structural design of B-pillar

In side impact, the injuries to organs in chest region more often result in fatality than injuries to the abdomen. Furthermore, a literature indicates that shoulder and thorax regions are more sensitive to velocity than abdomen^[8]. It seems that in protection of occupants we need in first hand reduce deformation of side car structure in the level of the chest region. Therefore, we desired deformation mode of B-pillar as "pendulum style"^[7]. This kind of mode requires that structure of B-pillar has high stiffness in the upper segment and low in the lower one. For this desired structure, a metal sheet with varying thickness is desirable. It not only reduces the amount of material but also increases design flexibility^[9]. So we used the TWB structure to replace the original one, in this way, the outer panel of B-pillar can be divided into two segments. As shown in Figure 5, the seam between these two segments was substituted by a simple boundary, which combined the nodes at borderline as common nodes, in the FE model.

Another interesting advantage of the application of the TWB structure is the possibility to reduce the number of components. In this case, in the key areas withstanding high stress we can apply high-strength material instead of thick sheets of reinforcements of original structure around this area^[2]. In the present study, the original B-pillar structure includes the outer panel, inner panel and reinforcements 1, 2, 3, 4, as shown in Figure 4. All these components of the B-pillar, except inner panel, were replaced by TWB structure. Therefore, the new B-pillar consists only of inner panel and outer panel, which is TWB structure.

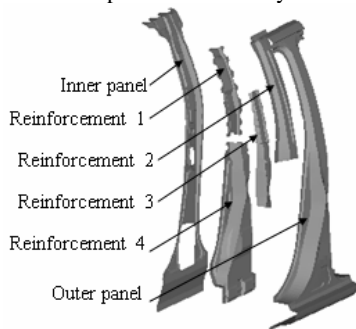


Figure 4. Components of B pillar structure

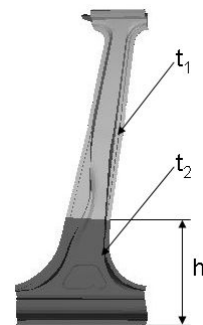


Figure 5. TWB structure of outer panel of B pillar

3 Multi-objective optimization problem description

3.1 Variables and objectives

As shown in Figure 5, the thickness of two segments (t_1 and t_2) and the location of seam (h) are chosen as the design variables, which could significantly affect the crashworthiness and light-weighting. We decided to investigate the influence of thickness of these two segments is range from 0.8 mm to 2.5 mm, which is the common thickness of automobile steel sheets. The location of the seam was chosen from 136 mm to 455 mm considering chest protection.

The side impact safety performance is usually evaluated by intrusion, intrusion velocity and intrusion mode^[6]. In our study,

B-pillar maximum intrusion (U), intrusion (L) and intrusion velocity (V) at the middle of inner panel of B-pillar were set as the design objectives for evaluation of crashworthiness. Moreover, the mass (M) of B-pillar was also chosen as the design objective for light-weighting. According to evaluation methods of B-pillar structural deformation that was made by the Insurance Institute for Highway Safety (IIHS), considering the vehicle structure size, there is 180mm space to deform inner panel under the situation that B-pillar structural deformation is still at the "excellent" level. Therefore we decided that B-pillar maximum intrusion (U) should be less than 180 mm. Generally speaking, the intrusion velocity range from 7 m/s to 10 m/s could be accepted in side impact. A literature indicates that it will be easy to satisfy the requirement of protection of the occupant in side impact if the intrusion velocity is less than 8 m/s [6]. So in current optimization the objective range of the intrusion velocity (V) in the middle of inner panel was set from 7 m / s to 8 m / s.

3.2 Multi-objective optimization problem

A general multi-objective optimization problem can be expressed as

$$\begin{aligned} \min F(X) &= [f_1(x), f_2(x), \dots, f_m(x)] \\ \text{s.t. } g_j(X) &\leq 0 \quad i = 1, 2, \dots, I \\ h_j(X) &\leq 0 \quad j = 1, 2, \dots, J \\ X &\in S \end{aligned} \quad (1)$$

where $f_1(x), f_2(x), \dots, f_m(x)$ are the m objective functions, $x = (x_1, x_2, \dots, x_n)^T$ are the n design variables, $x \in S$ defines the design space.

In the present study, this multi-objective mathematical model of optimization problem was defined as follows:

$$\begin{aligned} \min \{L, M\} \\ \text{s.t. } U &\leq 180\text{mm} \\ 7\text{m/s} &\leq V \leq 8\text{m/s} \\ 0.8\text{mm} &\leq t_1, t_2 \leq 2.5\text{mm} \\ 136\text{mm} &\leq h \leq 455\text{mm} \end{aligned} \quad (2)$$

4 Multi-objective optimization procedure

The whole multi-objective optimization method contains design of experiment (DOE), mathematical model regression and multi-objective genetic algorithm (GA). So the optimization procedure was divided in three steps. Firstly, we use the DOE method to obtain adequate design samples. Secondly, calculated the coefficients of mathematical models based on these samples. Finally, we optimized mathematical models by multi-objective GA.

4.1 Design of experiment

Design of experiments is a collection of procedures used to create a set of design samples. The generation of design samples can be done either pseudo-randomly according to a probability distribution or deterministically according to a predefined scheme. This set of samples is then commonly used as a set of support points for mathematical model regression or as stochastic realization for robustness evaluation [10].

Table1. The design samples

Sequence number	h [mm]	t_1 [mm]	Blank	t_2 [mm]	L [mm]	V [m/s]	U [mm]	M [Kg]
1	205	1	1	1	167 127	8.84383	207	7.168
2	205	1.6	2	1.6	113	7.17791	146.1	9.299
3	205	2.2	3	2.2	165	7.25814	128.9	11.43
4	302	1	2	1	138	8.92927	182.8	9.228
5	302	1.6	3	1.6	115	7.21126	171.5	8.269
6	302	2.2	1	1.6	178	7.18257	139.7	10.4
7	406	1	3	2.2	128	9.90218	192.4	8.36
8	406	1.6	1	1	130	7.55589	134.7	10.491
9	406	2.2	2	1		7.14635	171.1	9.045

In order to obtain adequate design samples, and then make it easy to establish mathematical model, in the present study the $L_9(3^4)$ orthogonal experiment design was chosen as shown in Table 1. For the randomly selected set of h , t_1 and t_2 we calculated V , M , L , and U from LS-Dyna simulations. Further all these results were used in calculation of the coefficients of mathematical models by the method of least squares.

4.2 Mathematical model regression

In response surface method, in order to develop a mathematical model that provides an explicit relationship between design variables and the objective of interest, we typically use first- or second-order models in the form of linear or quadratic polynomial functions. The unknown coefficients in the model are calculated using the method of least squares. The quadratic polynomial function, which is usually used, is shown as follow:

$$f(x) = \beta_0 + \sum_{i=1}^m \beta_i x_i + \sum_{i=1}^m \beta_{ii} x_i^2 + \sum_{i=1}^{m-1} \sum_{j=i+1}^m \beta_{ij} x_i x_j \quad (3)$$

Where $f(x)$ is the objective function, m is the total number of design variables, x_i is the i th design variable, and the β is the unknown coefficient of each polynomial term.

The major statistical parameters used for evaluation of model fitness are coefficient of determination R^2 and adjusted coefficient of determination R_{adj}^2 . Generally speaking, the closer the values of R^2 and R_{adj}^2 are to one, the error of mathematical model is smaller and the fit is better. In situations where the number of design variables is large, it is more appropriate to look at R_{adj}^2 , because R^2 always increases when the number of polynomial terms of the model is increased while R_{adj}^2 actually decreases if unnecessary terms are added to the model^[11].

In the present study, the quadratic polynomials for the regression are employed to represent the nonlinear responses of the B-pillar maximum intrusion (U), the intrusion (L) and intrusion velocity (V) at the middle of B-pillar inner panel, while a linear function is used in regression of the B-pillar mass (M). All the polynomial coefficients and fitness of the model were calculated in Excel. The functions obtained are as follows:

$$M = 3.616222 + 1.699722t_1 + 1.851944t_2 \quad (4)$$

$$U = 382.5351 + 0.16043h - 194.333t_1 - 61.8978t_2 - 0.08358ht_2 + 47.06213t_1^2 + 18.333t_2^2 \quad (5)$$

$$L = 267.3179 + 0.182366h - 160.91t_1 - 0.07412ht_2 + 8.7998t_1t_2 + 31.53953t_1^2 \quad (6)$$

$$V = 14.56747 + 0.011814h - 10.1768t_1 - 0.00486ht_2 + 1.023188t_1t_2 + 2.064668t_1^2 \quad (7)$$

It is essential to evaluate the accuracies of such mathematical models. In the present study we used both R^2 and R_{adj}^2 as a measure of the accuracy of the models. For M, U, L and V the R^2 is 0.994, 0.998, 0.997, 0.984 and the R_{adj}^2 is 0.992, 0.992, 0.993 and 0.956, respectively. Hence, the accuracies of the mathematical models are considered as adequate for the study.

4.3 Multi-objective genetic algorithm

The multi-objective evolutionary algorithm, named NSGA-II, is employed in the present study. In NSGA-II, a Pareto-based ranking of the existing designs in the population is applied for the stochastic selection process involved. As such, there exists a set of non-dominated designs for each population. Recall that, a design is Pareto-dominant when there is no other design in the population that is strictly better in terms of all objectives. As the search progresses from generation to generation, the non-dominated designs are driven gradually close to the true Pareto set of the problem. As a result, near-Pareto designs can be generated without putting together the different criteria into a single objective function using scaling weights^[12].

Based on these four mathematical models, the multi-objective optimization was performed using the NSGA-II algorithm by the iSIGHT software. The population size was chosen as 30, and the NSGA-II was running 100 generations.

5 Result and discussion

In the multi-objective optimization, it is often hardly possible to achieve all such objectives simultaneously. To some stage, any further improvement in one objective requires a tradeoff of at least one other objective. This defines a Pareto optimum, in which there exists no feasible solution that can decrease some objective functions without causing at least one other objective function to increase. In this sense, the Pareto optimum represents a set of solutions and a multi-objective approach leads to the identification of a Pareto set. The Pareto solution set obtained from iSIGHT software, which contains 30 Pareto's points, is shown in Table 2.

Table 2. Pareto solution set of multi-objective problem

Sequence number	L [mm]	U [mm]	M [kg]	V [m/s]
1	125.11	154.74	9.25	7.002
2	122.43	149.43	9.59	7.005
3	117.25	132.79	10.42	7.001
4	137.06	179.84	7.50	7.013
5	118.50	134.99	10.31	7.001
6	119.89	136.29	10.15	7.003
7	109.81	131.91	11.06	7.001
8	122.36	139.38	9.93	7.036
9	128.94	160.68	8.75	7.012
10	128.17	158.39	8.93	7.044
11	125.79	157.02	9.16	7.003
12	134.11	168.35	8.01	7.001
13	130.51	163.94	8.61	7.049
14	114.98	130.88	10.66	7.010
15	111.16	132.87	11.05	7.087
16	120.96	137.74	10.03	7.004
17	112.23	130.32	10.87	7.011
18	133.25	174.32	8.35	7.117
19	131.77	172.81	8.42	7.049
20	119.41	135.96	10.22	7.004
21	116.27	131.74	10.57	7.023
22	124.57	153.62	9.31	7.000
23	126.99	157.07	9.02	7.013
24	127.91	156.95	8.98	7.053
25	111.37	131.73	10.96	7.035
26	113.35	130.17	10.80	7.007
27	135.32	172.93	7.80	7.003
28	113.20	130.17	10.81	7.004
29	109.78	131.98	11.06	7.001
30	134.68	168.70	8.01	7.035

The present study aims to improve side impact safety performance while achieving light-weighting. Therefore considering the purpose of the study we choose the 9th, 10th, 13th, 23rd and 24th as the final solutions. The values of three variables of these final solutions are shown in Table 3.

Table 3. Variables of final solution [unit: mm]

Sequence number	t_1	t_2	h
9	1.103	1.818	320.75
10	1.148	1.874	336.18
13	1.053	1.789	321.49
23	1.165	1.909	337.12
24	1.179	1.874	336.18

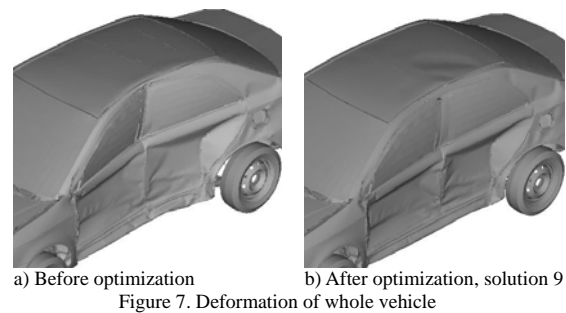
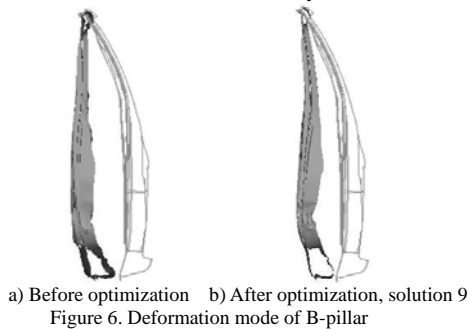
From Table 2 and Table 3, we can see that the values of both objectives and variables of the 9th and 13th, 10th, 23rd and 24th are similar, respectively. Therefore, only the 9th and 10th solutions found by the optimization procedure were taken into account in validation by LS-Dyna simulations. The two new models based on variables of these solutions were created and used in simulation of side impact. The simulation results of original and these new models, and also results predicted by optimization are shown in Table 4. In this table the improvement ratio that means the percentile expressed difference between simulation results using original design

and that using design after optimization are shown. At the same time, the errors between the results from simulation using the new model and these predicted by optimization are also shown. These errors are small, so that the multi-objective problem optimization results are valid.

Table 4. Validation results and effect of optimization

Objective	Original design	Solution 9				Solution 10			
		Optimization results	Simulation results	Error	Improvement ratio	Optimization results	Simulation results	Error	Improvement ratio
L [mm]	163	128.94	133	3.1%	18.4%	128.7	132	2.5%	19%
U [mm]	183.1	160.68	164.6	2.4%	10.1%	158.39	163.7	3.2%	10.6%
M [kg]	10.763	8.75	8.814	0.7%	18.1%	8.93	8.976	0.4%	16.6%
V [m/s]	8.255	7.012	7.28	3.7%	11.8%	7.044	7.36	4.3%	10.8%

As can be seen from Table 4, comparing optimization results with the original design, all values of objectives have been reduced obviously. Take the 9th solution as an example, B-pillar maximum intrusion (U) was reduced by 10.1%. The intrusion (L) and intrusion velocity (V) at the middle of B-pillar were reduced by 18.4% and 11.8%, respectively. The mass (M) was reduced by 18.1%. Meanwhile, the desired B-pillar deformation mode was obtained. The two deformation modes of B-pillar before and after optimization are shown in Figure 6 while Figure 7 shows the deformation of the whole vehicle. As shown in these two Figures, there is a significantly positive improvement of crashworthiness of side configuration. The maximum intrusion is not only reduced but also occurs in the level that is less dangerous for occupant considering injury risks. Figure 6 with the improvement of B-pillar also can be seen that the intrusions occurred by other side structures of vehicle are less.



One of the limitations of the study is that we decided to evaluate the influence of geometry of TWB structure on the crashworthiness and light-weighting. The influence of material properties was not considered. For the future work it could be a good idea to consider this factor in optimization and moreover to divide the B-pillar into three segments.

6 Conclusion

In the study we found that TWB structure with various stiffness used in B-pillar can obtain the desired deformation mode, enhance side impact safety performance, and at the same time the mass of vehicle and number of components will be reduced. This is due to the procedure of optimal designing of this structure applied in the study that can effectively balance the requirements of crashworthiness and light-weighting. The research methods and results of the study can be helpful at the early design stage to improve the vehicle body.

Acknowledgment

The research work was supported by the National 863 Program of China (NO.2006AA110101) and the "111 Plan" program (NO.111-2-11).

Reference

- [1] Marklund, P.O., Nilsson, L. (2001) Optimization of a car body component subjected to side impact. *Struct Multidisc Optim.* 21, pp. 383–392.
- [2] Zhu, P., Shi, Y.L., Zhang, K.Z and Lin, Z.Q. (2008) Optimum design of an automotive inner door panel with a tailor-welded blank structure. *Automobile Engineering*. Vol. 222 Part D, pp. 1337–1346.
- [3] Shin, J.K., Lee, K.H., Song, S.I., and Park, G.J. (2002) Automotive door design with the ULSAB concept using structural optimization. *Struct Multidisciplinary Optimization*. Vol. 23, pp. 320–327.
- [4] Lee, K.H., Shin, J.K., Song, S.I., Song, S.I., and Park, G.J. (2003) Automotive door design using structural optimization and design of experiments. *Automobile Engineering*. 217(10), pp. 855–865.
- [5] Song, S.I. and Park, G.J. (2006) Multidisciplinary optimization of an automotive door with a tailored blank. *Automobile Engineering*. 220(2), pp. 151–163.
- [6] Zhang, X.R and Su, Q.Z. (2008) A Research on Influencing Factors of Occupant Injury in Side Impact. *Automobile Engineering*.

- 30(2), pp. 146-150 (in Chinese).
- [7] Malkusson, R. and Karlsson, P. (1998) Simulation Method for Establishing and Satisfying Side Impact Design Requirements. SAE paper number 982358. pp. 1-7.
 - [8] Kalu, U., Wu, J.P., Sukbhir, B., Mark, G. and Murthy, K. (2005) Door Interior Trim Safety Enhancement Strategies for the SID-II's Dummy. SAE paper number 2005010284. pp. 1-10.
 - [9] Yang, R. J., Fu, Y. and Li, G. (2007) Application of Tailor Rolled Blank in Vehicle Front End for Frontal Impact. SAE paper number 2007010675. pp. 1-8.
 - [10] Bucher, C., Will, J. and Riedel, J. (2001) Multidisciplinary non-linear optimization with Optimizing Structural Language. 19th CAD-FEM Users' Meeting. pp. 1-11.
 - [11] Fang, H., Rais-Rohani, M., Liu, Z. and Horstemeyer, M.F. (2005) A comparative study of metamodeling methods for multi-objective crashworthiness optimization. Computers & Structures. 83, pp. 2121-2136.
 - [12] Liao, X.t., Li, Q., Yang, X.J., Zhang, W.G. and Li, W. (2008) Multi-objective optimization for crash safety design of vehicles using stepwise regression model. Struct Multidisc Optim. 35, pp. 561-569.